

# Limiting current on porous graphite electrodes under flow conditions

R. E. SIODA

*Institute of Physical Chemistry, Polish Academy of Sciences, Warszawa, ul. Kasprzaka 44, Poland*

Received 16 July 1974

The flow electrolysis of a solution of  $2.0 \times 10^{-3}$  M  $K_3Fe(CN)_6$  in 2 M KCl in water on porous graphite electrodes is described. The electrodes have been composed of crushed graphite of three grain size ranges:  $0.7 \div 1.0$ ,  $0.4 \div 0.7$ , and  $0.25 \div 0.4$  mm. Electrodes of three different heights have been investigated, and the solution flow rate ranged between  $0.009$  and  $0.25$  ml  $s^{-1}$ . The dependence of the logarithm of the limiting current and of the limiting degree of conversion on the logarithm of the flow rates is shown for the electrodes. The obtained experimental results are interpreted by means of the described earlier semi-empirical model of the limiting current on flow-through porous electrodes.

## 1. Introduction

Porous graphite electrodes are promising for use in flow electrochemical cells and reactors. They are easily available and suitable for work with different types of solvents; this is specially important in the field of preparative organic reactions. The application of porous graphite electrodes for flow cells has been already described [1–4]. In experiments with these electrodes, limiting currents have been observed [2], indicating mass-transfer limitations to the internal surface. A semi-empirical model of limiting currents on porous electrodes under conditions of flow has been described by the present author, and was satisfactorily applied to flow cells with porous electrodes composed of fine platinum grid [5–8]. In the present paper the model is applied to analysis of experimental limiting currents obtained on porous graphite flow-through electrodes. Recently, Wroblowa and Razumney described a model of the limiting current based on a capillary bundle model of a porous media; calculations done according to this model compared favourably with the present author's earlier experimental results [9]. However the model of Wroblowa and Razumney is complicated mathematically, and for a practical task of a simple description of experimental results the semi-empirical model of the present author seems more convenient.

## 2. Experimental

### 2.1. The cell

A cell has been employed similar to that shown before [2], with the exception that the working electrode was contained in a straight piece of glass tube (internal diameter 4.0 mm, open cross-section area  $a = 0.126$  cm<sup>2</sup>) without a thinning beneath the electrode. 80-mesh platinum grid was fused into the light of the tube as a support for the graphite electrode. Three sieve fractions of a crushed spectrographic graphite were used for preparing electrodes. The fractions denoted *A*, *B*, and *C* contained granules in the following size ranges: *A*,  $0.7 \div 1.0$ ; *B*,  $0.4 \div 0.7$ ; and *C*,  $0.25 \div 0.4$  mm. The measured medium weights of granules in the fractions were: *A*,  $3.1 \times 10^{-4}$ , *B*,  $8.5 \times 10^{-5}$ ; and *C*,  $1.3 \times 10^{-5}$  g. From these the following medium equivalent diameters of the granules were calculated: *A*, 0.068; *B*, 0.044; and *C*, 0.024 cm for the measured apparent density of graphite  $\rho_{gr} = 1.9$  g cm<sup>-3</sup>. The three graphite fractions gave practically the same bed density of  $0.75$  g cm<sup>-3</sup>, corresponding to an apparent porosity of macropores  $\epsilon = 0.61$ . To increase the electric conductance of the graphite beds, a small piece of platinum wire of 0.2 mm in diameter was put through them. The electrolyses were conducted against a platinum

counter-electrode, located above the working electrode (up the flow). The potential of the working electrode was measured against a saturated calomel electrode placed beneath the working electrode (down the flow). Both the counter- and reference electrodes were separated from the flow system by filter paper plugs. The flow of the solution was gravitational. The flow rate was regulated by attaching capillaries of different diameters to the outlet of the cell. It was measured by collecting volumes of the effluent in time intervals. The electrolyzed solution was de-aerated before the experiments by bubbling nitrogen. The measurements were conducted at room temperature of 22°C.

## 2.2. Chemicals

The salts employed have been of analytical purity. The investigated solution of  $2.0 \times 10^{-3}$  M  $K_3Fe(CN)_6$  and 2 M KCl in doubly distilled water had density  $\rho_{sol} = 1.089$  g cm $^{-3}$ , and viscosity  $\mu = 0.97$  centipoise at 22°C.

## 3. Results

As before, the process of the electroreduction of a solution of  $2.0 \times 10^{-3}$  M  $K_3Fe(CN)_6$  in a supporting electrolyte of 2 M KCl in water was employed for studying the properties of the limiting currents on the graphite electrodes. The electric conditions which have to be satisfied for obtaining a limiting current on a porous electrode were described earlier [6]. In the experiments only a single potential value was measured for the graphite beds; it was assumed that the potential drop in the beds was negligible due to the high concentration of the supporting electrolyte, and hence mass-transfer control of the electrolytic process occurred practically concurrently in the whole volume of the electrode. The validity of the above assumption is confirmed by Fig. 1, where voltammetric curves of the reduction of  $K_3Fe(CN)_6$  are shown for three electrodes, each composed of 0.054 g of graphite (electrode heights  $L \cong 0.57$  cm) of one of the three fractions, at the same flow rate  $v = 0.105$  ml s $^{-1}$ . On the curves are seen well developed limiting current regions — extending for about 1 V — corresponding to the mass-transfer control of the electrolytic process. As expected, the highest limiting current is obtained for the

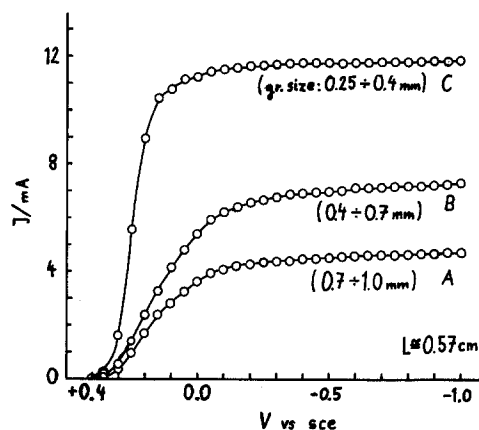


Fig. 1. The voltammetric curves of the reduction of  $2.0 \times 10^{-3}$  M  $K_3Fe(CN)_6$  in 2 M KCl in water for three porous electrodes of length  $L \cong 0.57$  cm, composed of graphite granules of fractions A, B and C (curves A, B and C respectively, grain size ranges shown). The solution flow rate,  $v = 0.105$  ml s $^{-1}$ .

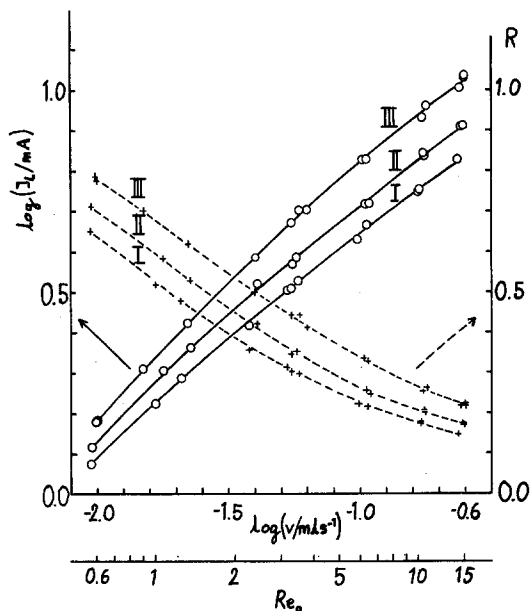


Fig. 2. The dependence of the limiting current (solid curves, lefthand ordinate) of the reduction of  $2.0 \times 10^{-3}$  M  $K_3Fe(CN)_6$  in 2 M KCl in water, and of the corresponding limiting degrees of conversion (dotted curves, right-hand ordinate) on the flow rate. The electrodes have been composed of graphite fraction A, and had following heights: I,  $L \cong 0.57$ , II, 0.85 and III, 1.05 cm. The scale of modified Reynolds Numbers,  $Re_0$ , is given below.

electrode composed of the smallest granules, i.e. of fraction C. The ratio of magnitudes of the limiting currents in Fig. 1 at  $-0.5$  V versus sce for fractions A, B, and C respectively is 1:1.55:2.60.

The apparent differences in the slopes of the three curves are caused by individual differences in the ohmic resistances of the beds.

The dependences of the magnitudes of limiting current on the flow rate, on the electrode height, and on the average granule size have been investigated. Magnitudes of the limiting current were measured at constant potential of  $-0.5$  V versus reference sce after stabilization of the current lasting usually less than 1 min. In Fig. 2 are shown in logarithmic coordinates the measured dependences of the limiting current on the flow rate for electrodes composed of graphite fraction *A* of three heights:  $L \cong 0.57, 0.85$  and  $1.05$  cm (heights calculated from masses of the beds respectively equal  $0.054, 0.080$  and  $0.099$  g). The experimental points lie on curves of small curvatures, resembling straight lines of increasing slopes with increasing height of the electrode. This is in qualitative agreement with earlier observations [2]. In Fig. 2 are also given (dotted curves) the corresponding dependences of the limiting degree of conversion on the logarithm of the flow rate. The limiting degree of conversion in the flow electrolysis,  $R$ , is defined as the degree of conversion of substrate corresponding to an electrolysis with a limiting current [5–7, 10]:

$$R = \frac{I_1}{nFc_0v}, \quad (1)$$

where  $I_1$  is the limiting current,  $n$  the number of electrons transferred per molecule of substrate,  $F$  Faraday,  $c_0$  the initial concentration of substrate, and  $v$  the volume flow rate.

Similar dependences have been done for electrodes composed of the two graphite fractions *B* and *C*, and the results are presented in Fig. 3. Curves *IV* and *V* correspond to electrodes composed of fraction *B* of graphite content respectively  $0.054$  and  $0.080$  g (electrode heights:  $L \cong 0.57$  and  $0.85$  cm). Curve *VI* was measured for an electrode composed of graphite fraction *C* of graphite content  $0.054$  g (electrode height  $L \cong 0.57$  cm). The shapes of the curves are similar to that of the curves in Fig. 2, but the currents are generally higher, corresponding to higher limiting degrees of conversion (dotted curves).

In Figs. 2 and 3 are given the scales of modified Reynolds Numbers corresponding to the applied flow rates ranges, taking into account the medium equivalent diameters of the granules. The modified

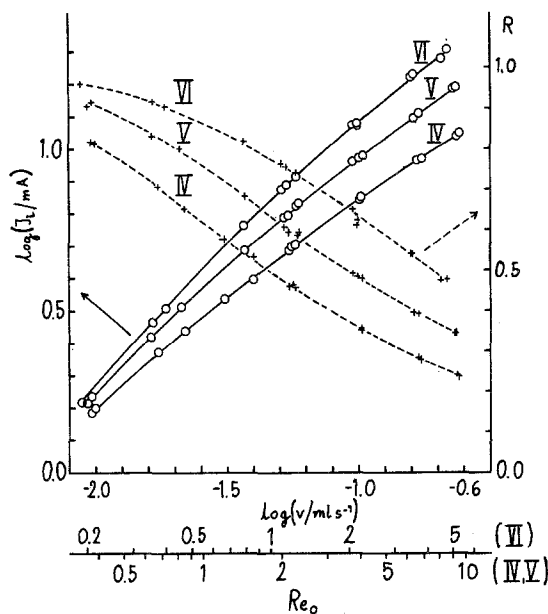


Fig. 3. The dependence of the limiting current (solid curves, lefthand ordinate) of the reduction of  $2.0 \times 10^{-3}$  M  $K_3Fe(CN)_6$  in 2 M KCl in water, and of the corresponding limiting degrees of conversion (dotted curves, right-hand ordinate) on the flow rate. Curves *IV* and *V* correspond to electrodes composed of graphite fraction *B* of following lengths: *IV*,  $L \cong 0.57$ , and *V*,  $0.85$  cm. Curve *VI* corresponds to the electrode composed of graphite fraction *C* of length  $L \cong 0.57$  cm. Scales of modified Reynolds Numbers,  $Re_0$ , are given below.

Reynolds Numbers,  $Re_0$ , have been calculated according the the formula [11]:

$$Re_0 = \frac{vd\rho_{sol}}{a\mu}, \quad (2)$$

where  $d$  is the average particle diameter. The calculated modified Reynolds Numbers are in all experiments smaller than 15. Accordingly it seems that the applied flow rates correspond to laminar flow region, or the beginning of transition flow region, as for turbulent flow in packed beds higher modified Reynolds Numbers are expected [12].

The limiting currents for the supporting platinum grid and the conducting wire alone have been small in comparison with limiting currents for the beds. In the case of the electrode, which gave the smallest currents, i.e. composed of graphite fraction *A* and of height  $L \cong 0.57$  cm, the supporting platinum grid and wire were responsible for about 5–7% of the degree of conversion of the flowing substrate. For electrodes of bigger height or composed of smaller granules (fractions *B* and *C*) the

relative participation of the current on grid and wire in the overall reduction process has been even smaller, and could be practically neglected.

#### 4. Discussion

The foundations of the semi-empirical model of the limiting current in the flow electrolysis on porous electrodes have been already described [5–8], and presently the model can be applied to the investigated beds of granulated graphite. According to the model, provided that dispersion in the bed can be neglected, the following equation should apply:

$$\log \log [1/(1-R)] = \log M + \log (jsLa^{1-\alpha}) + (\alpha - 1) \log v, \quad (3)$$

where  $M = \log e = 0.4343$ ,  $s$  is the specific surface of the bed, and  $j$  and  $\alpha$  are empirical mass-transfer constants,  $\alpha$  being a fraction of one. As the electrode specific surface is not always known, a characteristic constant  $b$  is introduced where  $b = js$ . The empirical parameters  $b$  and  $\alpha$  can be determined from a plot of the dependence of  $\log \log [1/(1-R)]$  versus  $\log v$  where the limiting degree of conversion  $R$  is calculated according to Equation 1. Such plots prepared from the limiting currents of Figs. 2 and 3 are shown respectively in Figs. 5 and 6. In all cases straight lines have been obtained:

$$\log \log [1/(1-R)] = A + B \log v, \quad (4)$$

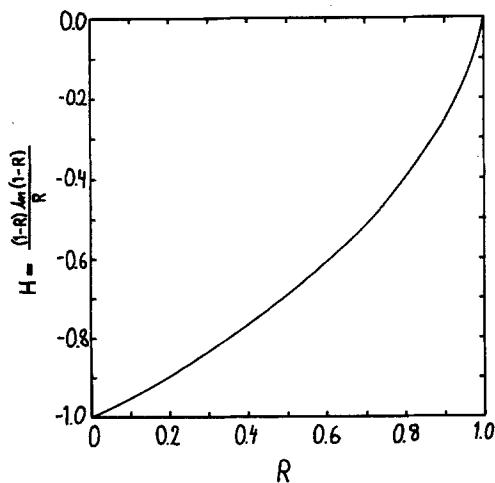


Fig. 4. The calculated dependence of the function  $H = [(1-R)\ln(1-R)]/R$  from Equation 8 on the limiting degree of conversion  $R$ .

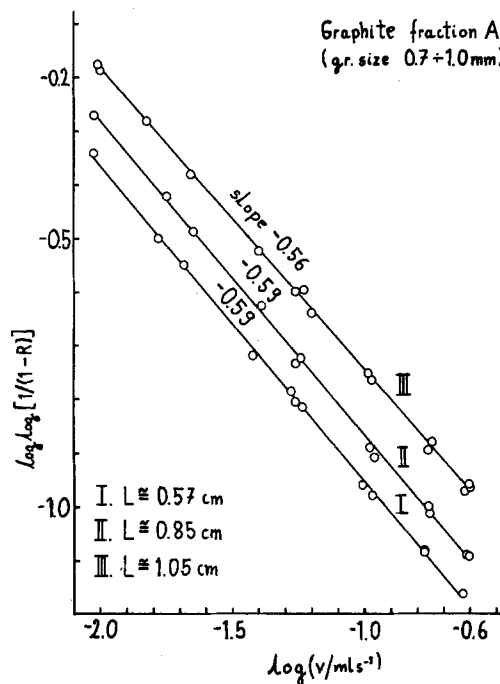


Fig. 5. The dependence of  $\log \log [1/(1-R)]$  on  $\log v$  calculated for the limiting currents given in Fig. 2.

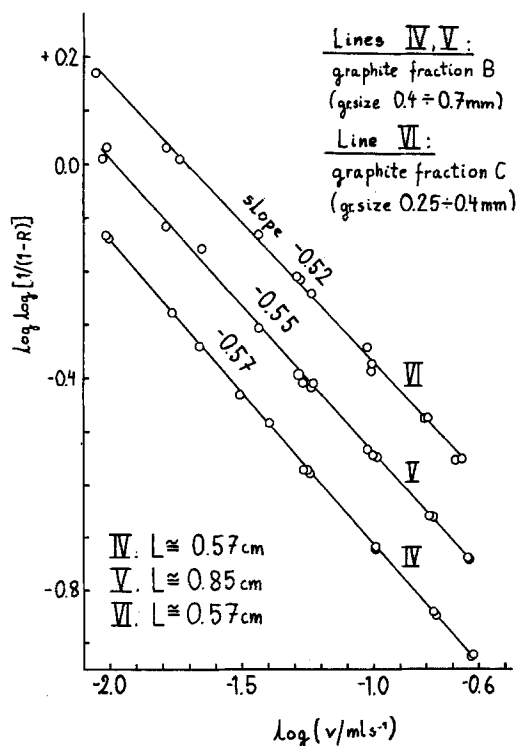


Fig. 6. The dependence of  $\log \log [1/(1-R)]$  on  $\log v$  calculated for the limiting currents given in Fig. 3.

Table 1. Intercepts *A* and slopes *B* of the lines in Figs. 5 and 6, and calculated values of the parameters  $\alpha$  and  $b = js$

Line number	<i>A</i>	<i>B</i>	$r^{2*}$	Standard deviations		Calculated	
				<i>A</i>	<i>B</i>	$\alpha$	<i>b</i>
				(%)			
I	-1.542	-0.589	0.999	0.5	1.0	0.411	0.39
II	-1.455	-0.587	0.998	1.3	1.2	0.413	0.32
III	-1.308	-0.563	0.999	0.5	0.9	0.437	0.34
IV	-1.284	-0.570	0.9997	0.3	0.5	0.430	0.68
V	-1.092	-0.550	0.999	0.6	0.9	0.450	0.68
VI	-0.895	-0.524	0.997	1.1	1.5	0.476	1.52

\* Square of coefficient of correlation.

whose intercepts (*A*) and slopes (*B*) determined by least-squares method are presented in Table 1. From the slopes and intercepts of the lines the empirical parameters  $b = js$  and  $\alpha$  in Equation 3 have been determined, and their calculated values are also given in Table 1. In agreement with the model, the empirical parameters *b* and  $\alpha$  are approximately constant despite changing the height of the porous electrode. The average values of the parameters for the graphite fractions *A* and *B* are respectively:  $\alpha = 0.42 \pm 0.02$ ,  $b = 0.35 \pm 0.04$ , and  $\alpha = 0.44 \pm 0.01$ ,  $b = 0.68 \pm 0.01$ . Although for the fraction *C* limiting currents for only one electrode height,  $L \cong 0.57$  cm (corresponding to graphite mass 0.054 g), have been measured, the measurements have been repeated several times, and the obtained values of  $\alpha = 0.48$  and  $b = 1.52$  are reliable. As follows from Table 1,  $\alpha$  increases somewhat the higher the electrode, or the smaller is the diameter of granules. This effect may be caused by the dispersion of substrate in the electrode. It will be discussed later in the paper.

The ratio of the determined average *b* constants for the graphite fractions *A*, *B* and *C* is respectively:  $0.35 : 0.68 : 1.52 = 1 : 1.9 : 4.3$ . According to the applied model, *b* is equal to a product of the mass-transfer constant *j* and of the specific surface of the bed *s*,  $b = js$ . If by analogy with a bed composed of spheres we assume that the specific surface is inversely proportional to medium equivalent diameters of granules, the specific surfaces of the three graphite fractions *A*, *B* and *C* should form the ratio:  $1 : 1.55 : 2.83$ . This ratio is smaller than the given above ratio of the determined *b* constants, especially for the fraction *C*. It seems that this may be due to an increase of the mass-transfer constant *j* for small granules, and consequently for small diameters of capillaries

between them. This effect should become significant when the medium diameter of capillaries is comparable or smaller than the Nernst diffusion layer thickness. Similar effect of 'abnormal' increase of the mass-transfer for very small capillaries has been observed by Blaedel and Boyer in their study of electrolysis on flow-through micromesh electrodes [13]. If the average granule diameters of the fractions *A*, *B* and *C* are taken as the average of granule size ranges, the following ratio of the specific surfaces should be obtained:  $1 : 1.55 : 2.62$ .

Again the ratio is smaller than the ratio of the experimentally determined *b* constants for the three fractions.

#### 4.1. Approximate determination of the parameter $\alpha$

The approximate value of the parameter  $\alpha$  can in principle be determined from a plot of the dependence of  $\log I_1$  on  $\log v$ , as in Figs. 2 and 3. According to the applied model of the flow electrolysis on porous electrodes, the limiting current,  $I_1$ , is given by the following equation [5]:

$$I_1 = nFc_0vR = nFc_0v[1 - \exp(-ba^{1-\alpha}v^{\alpha-1}L)]. \tag{5}$$

After taking a logarithm of both sides of Equation 5, differentiation with respect to  $\log v$ , and rearranging, the following dependence is obtained:

$$m = \frac{d}{d \log v} (\log I_1) = 1 + \frac{(1-R)\ln(1-R)}{R} (1-\alpha). \tag{6}$$

Equation 6 can be transformed to a following form suitable for determination of  $\alpha$ :

Table 2. Parameter  $\alpha$  calculated from the slopes of the solid curves in Figs. 2 and 3 at  $\log(v/\text{ml s}^{-1}) = -1.3$

Curve	$m$	$R$	$H$	$\alpha$
I	0.51	0.32	-0.82	0.40
II	0.55	0.37	-0.79	0.43
III	0.60	0.46	-0.72	0.44
IV	0.60	0.48	-0.71	0.44
V	0.67	0.60	-0.61	0.46
VI	0.77	0.76	-0.45	0.49

$$\alpha = 1 + \frac{1-m}{H} \quad (7)$$

where  $m$  is the slope of the dependence of  $\log I_1$  on  $\log v$  at given value of  $\log v$ , and  $H$  is a following function of the limiting degree of conversion at that point:

$$H = \frac{(1-R)\ln(1-R)}{R} \quad (8)$$

The calculated dependence of  $H$  on  $R$  is presented in Fig. 4. The application of Equation 7 to solid curves of Figs. 2 and 3 at a constant value of  $\log(v/\text{ml s}^{-1}) = -1.3$  led to results given in Table 2. The slopes and the limiting degrees of conversion in Table 2 have been determined graphically. It is seen that thus calculated approximate values of  $\alpha$  are close to those determined before and presented in Table 1.

#### 4.2. Dispersion in the porous electrodes

It is known that packed-bed reactors exhibit the effect of dispersion, consisting of mixing the solution in the bed due to combined molecular diffusion and fluid mechanical forces [11]. A mathematical model of reactor with dispersion, constructed by Danckwerts [14], has been applied by the present author to construct a model of a porous flow-through electrode [7, 8]. According to this model, provided that dispersion coefficient is small, the limiting degree of conversion for a porous electrode is equal:

$$R = 1 - (1 + b^2 D^* L a^{3-2\alpha} v^{2\alpha-3}) \times \exp(-b L a^{1-\alpha} v^{\alpha-1}), \quad (9)$$

where  $D^*$  is the effective coefficient of dispersion equal to the product of the coefficient of longitudinal dispersion,  $D_L$ , and porosity,  $D^* = D_L \epsilon$ . The effect of dispersion lowers the degree of

conversion in comparison with that expected for an ideal reactor based on a plug flow approximation. According to existing theories the coefficient of longitudinal dispersion depends following on the solution flow rate, and on the diameter of particles forming the bed [11]:

$$D_L = \frac{vd}{2a\epsilon} \quad (10)$$

As has already been said, the small increase of the slopes in Figs. 5 and 6 with the decrease of the granule size and with the increase of height of electrode (both factors increase the limiting degree of conversion) may be caused by the effect of dispersion. An analysis of Equation 9 is presented below showing an approximate method of estimating the magnitude of the coefficient of dispersion from the slopes of the lines in  $\log \log [1/(1-R)]$  versus  $\log v$  plots.

Equation 9 can be transformed to the following form:

$$\log \log [1/(1-R)] = \log [M b L a^{1-\alpha} v^{\alpha-1} - \log(1 + b^2 D^* L a^{3-2\alpha} v^{2\alpha-3})] \quad (11)$$

This equation is differentiated with respect to  $\log v$ , assuming that  $D^*$  is a constant, and substituting  $v = 10^{\log v}$ . The resulting equation is simplified with help of Equation 9, and  $D^*$  is calculated:

$$D^* = D_L \epsilon = \frac{(1-R)[(1-\alpha)bLa^{1-\alpha}v^{\alpha-1} - \beta \ln(1-R)]}{(3-2\alpha)b^2La^{3-2\alpha}v^{2\alpha-3} \exp(-bLa^{1-\alpha}v^{\alpha-1})}, \quad (12)$$

where  $\beta$  is the derivative

$$\frac{d}{d \log v} \{ \log \log [1/(1-R)] \}.$$

In order to use Equation 12 the parameters  $\alpha$  and  $b$  must be known. It seems that  $\alpha$  should depend primarily on the type of the flow (laminar or turbulent). By analogy with electrodes of simple geometrical shapes like wires, spheres, cones and grids placed in flow [5, 15], it is supposed that values of  $\alpha$  between 0.3 and 0.5 correspond to laminar flow region. Higher values of  $\alpha$  (above 0.5) are expected for turbulent flow. Another factor which may influence  $\alpha$  is the internal geometry of

Table 3. Longitudinal dispersion coefficients  $D_L$  calculated from the slopes of the lines III and VI in Figs. 5 and 6 and independently by Equation 10

Line (number)	$\bar{v}/\text{mls}^{-1}$ *	$D_L/\text{cm}^2\text{s}^{-1}$ (slopes, Equation 12)	$D_L/\text{cm}^2\text{s}^{-1}$ (Equation 10)
III	0.065	0.017	0.029
IV	0.056	0.008	0.016
V	0.058	0.018	0.016
VI	0.063	0.015	0.010

\* Flow rate corresponding to mean value of  $\log v$  of experimental points of the lines. These values have been substituted in Equations 10 and 12.

the electrode. For porous electrodes built of rolled together or parallel 80-mesh platinum wire grids,  $\alpha$  has been determined to equal 0.373 in a broad range of flow rates [7, 8]. In the present case of electrodes built of irregular granules,  $\alpha$  may be different from the above value, but in the first approximation, independent of the diameter of the granules. It seems reasonable to suppose that for the graphite granules the real value of  $\alpha$ , independent of dispersion effects, should be close to the smallest value determined from the  $\log \log [1/(1-R)]$  versus  $\log v$  plots, i.e.  $\alpha = 0.413$ . Hence a value  $\alpha = 0.41$  will be adopted in the calculation of the dispersion coefficients. As it has been found that the parameter  $b$  is rather insensitive to small changes of  $\alpha$ , its values from Table 1 have been used in the calculation of dispersion. Further, the slopes  $B$  given in Table 1 have been substituted for the values of the derivative  $\beta$ , and flow rates have been used corresponding to mean values of  $\log v$  for the points of the lines in Figs. 5 and 6. Thus calculated values of the approximate dispersion coefficients for lines III + VI are given in Table 3. They are compared with the expected values calculated according to Equation 10. From the comparison it is seen that the two independent calculations lead to values of the same order of magnitude, although quantitative agreement is not obtained. In the derivation of Equation 12 an approximation has been done that  $D^*$  is a constant not dependent on  $\log v$ . When the dependence of  $D^*$  on  $v$  according to Equation 10 is adopted before the differentiation, an equation similar to Equation 12 is obtained differing only by a multiplying factor  $(2\alpha - 3)/(2\alpha - 2)$ . For  $\alpha = 0.41$ , this factor becomes equal 1.85. Thus according to this approach, the dispersion coefficients calculated from the slopes of the lines will be higher by a

factor of 1.85 than the former values. This does not lead to better quantitative agreement with values calculated according to Equation 10.

## 5. Conclusions

The obtained results indicate that the semi-empirical model of the limiting current in the flow electrolysis on porous electrodes is applicable both to electrodes built of grids as well as to electrodes composed of granules of irregular shape. Due to its simplicity, the model can be of a help in mathematical description of flow electrolytic experimental data, and especially in calculations connected with an application of porous electrodes for electropreparations and for electroanalysis. The empirical parameters of the model can be easily determined by the methods described. Primarily the model describes the dependence of the limiting current and corresponding to it limiting degree of conversion on such experimentally important parameters such as flow rate and electrode length. The dependence of the limiting current and of the limiting degree of conversion on the specific surface of the electrode, although included in the model is in practical situations more complicated, as for electrodes of high specific surface concurrent change of the mass-transfer parameter  $j$  can be expected. At high degrees of conversion obtained especially on electrodes of high specific surface, the dispersion effects may become significant. A method is described of calculation of approximate dispersion coefficients from the slopes of  $\log \log [1/(1-R)]$  versus  $\log v$  plots. It has been found that dispersion coefficients calculated by this method from the slopes of the lines in Figs. 5 and 6 are of the same order of magnitude, as those calculated independently by Equation 10.

This agreement substantiates the assumption that dispersion is mainly responsible for changing the slopes of the lines with increasing specific surface or height of the electrode.

### References

- [1] W.J. Blaedel and J.H. Strohl, *Analyt. Chem.* **36** (1964) 1245.
- [2] R.E. Sioda, *Electrochim. Acta* **13** (1968) 1559.
- [3] R.I. Bamberger and J.H. Strohl, *Analyt. Chem.* **41** (1969) 1450; J.H. Strohl and T.A. Polutanovich, *Anal. Lett.* **2** (1969) 423.
- [4] H.S. Wroblowa and A. Saunders, *J. Electroanalyt. Chem.* **42** (1973) 329.
- [5] R.E. Sioda, *Electrochim. Acta* **15** (1970) 783.
- [6] *Ibid* **16** (1971) 1569.
- [7] *Ibid*, *J. Electroanalyt. Chem.* **34** (1972) 411.
- [8] *Ibid*, *Electrochim. Acta* **17** (1972) 1939.
- [9] H.S. Wroblowa and G. Razumney, *J. Electroanalyt. Chem.* **49** (1974) 355.
- [10] R.E. Sioda, *Electrochim. Acta* **13** (1968) 375.
- [11] J.M. Coulson and J.F. Richardson, 'Chemical Engineering', Vol. II, Pergamon Press, 1968.
- [12] R.E. Collins, 'Flow of fluids through porous media', Reinhold Publishing Corporation, New York, 1961, p. 51.
- [13] W.J. Blaedel and S.L. Boyer, *Analyt. Chem.* **45** (1973) 258.
- [14] P.V. Danckwerts, *Chem. Engng. Sci.* **2** (1953) 1.
- [15] V.G. Levich, 'Physical Hydrodynamics', Prentice-Hall, Englewood Cliffs, N.J., 1962.